Hidden symmetry in passive scalar advected by two-dimensional Navier-Stokes turbulence

Chiara Calascibetta,[1,*] Luca Biferale,[2,3] Fabio Bonaccorso,[2,3]
Massimo Cencini,[4,3] and Alexei A. Mailybaev[5]
[1]*Université Côte d'Azur, Inria, Calisto team, 06902 Sophia Antipolis, France*
[2]*Department of Physics, University of Rome "Tor Vergata", Via della Ricerca Scientifica 1, 00133 Rome, Italy*
[3]*INFN, Sezione di Roma "Tor Vergata", Rome, Italy*
[4]*Istituto dei Sistemi Complessi, CNR, Via dei Taurini 19, 00185 Rome, Italy*
[5]*Instituto de Matemática Pura e Aplicada– IMPA, Rio de Janeiro, Brazil*

(Received 16 April 2025; accepted 9 July 2025; published 26 August 2025)

Here we show that passive scalars possess a hidden scaling symmetry when considering suitably rescaled fields. Such a symmetry implies (i) universal probability distribution for scalar multipliers and (ii) Perron-Frobenius scenario for the anomalous scaling of structure functions. We verify these predictions with high resolution simulations of a passive scalar advected by a 2D turbulent flow in inverse cascade.

DOI: 10.1103/hfqj-py5v

I. INTRODUCTION

Scalar fields transported by turbulent flows are encountered in many natural and engineering settings, from atmospheric dynamics [1] to combustion [2]. Passive scalar statistics exhibit intermittency with universal anomalous scaling exponents, independent of the injection mechanism [3,4]. Kraichnan's insigths that passive scalar in Gaussian and time-uncorrelated flows can be intermittent [5] led to breakthroughs [6–8] that, exploiting the linearity of the advection equation, linked intermittency to the anomalous scaling of zero modes, homogeneous solutions of the scalar multipoint correlation functions. Zero modes, originally derived by perturbative expansions in the Kraichnan model (see also [9–11]), are statistically preserved structures of the Lagrangian dynamics [4]. Universality and statistical preservation under Lagrangian dynamics were then verified in realistic flows [12–14], such as scalars advected by 2D turbulence in the inverse cascade, which is nonintermittent [15]. After more than twenty years, however, the zero-mode picture of anomalous scaling did not allow to advance our understanding of anomalous scaling in Navier-Stokes (NS) 3D turbulence [16] nor in active scalars [17].

Recently, it was proposed that NS equations and, similarly, shell models for turbulence possess a hidden symmetry (HS) [18–21] (the existence of HS in turbulence was somehow conjectured in [22,23]), namely become scale invariant when considering suitably (nonlinearly) rescaled fields, which are thus nonintermittent. Notably, HS provides theoretical support to the universality of multiplier statistics, as conjectured by Kolmogorov third hypothesis [24] (see also [25]) and a way to link anomalous scaling to the eigevalues of a Perron-Frobenious operator [18], also offering support to the multiplicative view of intermittency and the multifractal model [26]. Very recently, HS was extended to a shell-model version of Kraichnan's model [27], previously rationalized within the zero modes framework [28,29]. Such results suggest the possibility of bridging HS with zero modes.

*Contact author: chiara.calascibetta@inria.fr

 ©2025 American Physical Society

In this manuscript, we demonstrate that realistic models of passive scalar turbulence also possess the hidden symmetry. We do so by considering a homogeneous and isotropic passive scalar advected by 2D NS turbulence in the inverse cascade [12–14], for which we numerically verify the universality of scalar multipliers, extending the Kolmogorov third hypothesis to scalar turbulence, and the Perron-Frobenius approach to anomalous exponents.

II. PASSIVE SCALAR IN 2D TURBULENCE

We consider the advection-diffusion equation for a passive scalar field, θ, in two dimensions

$$\partial_t \theta + \mathbf{v} \cdot \nabla \theta = \kappa \Delta \theta + f_\theta, \tag{1}$$

where κ is the scalar diffusivity, and f_θ is a Gaussian forcing applied at large scales [13]. The velocity field, $\mathbf{v}$, obeys the incompressible 2D NS equations

$$\partial_t \mathbf{v} + (\mathbf{v} \cdot \nabla)\mathbf{v} = -\nabla p + \nu \Delta \mathbf{v} - \beta \mathbf{v} + \mathbf{f}, \tag{2}$$

with p the pressure, ν the kinematic viscosity, and β a large-scale friction term preventing large-scale energy accumulation, due to the inverse energy cascade, which is sustained by a small scale Gaussian forcing, $\mathbf{f}$. Appendix A details the numerical implementation.

As well established in experiments and numerical simulations [15,30,31], in 2D inverse cascade, the velocity field is scale invariant with Kolmogorov scaling. In other words, within the inertial range, the velocity field exhibits the space-time scaling symmetry $\mathbf{x},\ t,\ \mathbf{v} \mapsto \gamma \mathbf{x},\ \gamma^{2/3} t,\ \gamma^{1/3}\mathbf{v}$ for $\gamma > 0$, which is admitted by Eq. (2) with $\nu = \beta = \boldsymbol{f} = 0$. Actually (as discussed below), such scale invariance applies to velocity differences rather than the velocity field itself due to the sweeping effect. Even with scale invariant velocity fields, the advected scalar exhibits intermittency [3,4]. As a result, for passive scalars, an extra relation $\theta \mapsto \gamma^\alpha \theta$, with arbitrary $\alpha \in \mathbb{R}$, adds to the space-time scaling symmetry, leading to a broader family of symmetries. Indeed, the stationary probability measure exhibits statistical intermittency in the form of multifractal scaling [26]. Intermittency reveals in the statistics of scalar increments

$$\delta_\ell \theta(\mathbf{x}, \mathbf{R}, t) = \theta(\mathbf{x} + \ell \mathbf{R}, t) - \theta(\mathbf{x}, t), \tag{3}$$

usually used with a direction vector $\mathbf{R} = \mathbf{e}$. As found in [13] and further illustrated in Fig. 1(b), the normalized probability density functions (PDFs) of $\delta_\ell \theta$ fail to collapse at different scales $\ell_n = 2^{-n}$ and deviate from Gaussianity. The lack of self-similarity is linked to the sharp gradients (cliffs) and smooth regions (ramps) characterizing turbulent scalar transport [3,13], which are exemplified in Fig. 1(a).

III. HIDDEN SYMMETRY FOR PASSIVE SCALAR

We now introduce the hidden symmetry framework, a general approach designed to transform an intermittent field into a nonintermittent one by identifying a suitable change of variables [18–21,27]. While this framework can be applied to any intermittent field, here we focus on the passive scalar in 2D turbulence and seek a transformation that eliminates the aforementioned dependence on α in the scaling symmetry, underlying the observed intermittency. We first demonstrate that the Kolmogorov scaling symmetry of velocity increments, $\delta_\ell \mathbf{v}(\mathbf{x}, \mathbf{R}, t) = \mathbf{v}(\mathbf{x} + \ell \mathbf{R}, t) - \mathbf{v}(\mathbf{x}, t)$, can be reformulated as a symmetry of the equations of motion in the quasi-Lagrangian (QL) frame, removing the sweeping effect. The approach is then exported to the passive scalar field.

Let the Lagrangian tracer $\mathbf{x}_\star(t)$, solving $d\mathbf{x}_\star/dt = \mathbf{v}(\mathbf{x}_\star, t)$, be the moving origin in the QL formulation and fix a reference scale ℓ within the inertial range [see sketch in Fig. 1(a)]. Together, these quantities define the rescaled QL coordinates [32]:

$$\mathbf{R} = (\mathbf{x} - \mathbf{x}_\star(t))/\ell, \quad \tau = t/t_\ell, \tag{4}$$

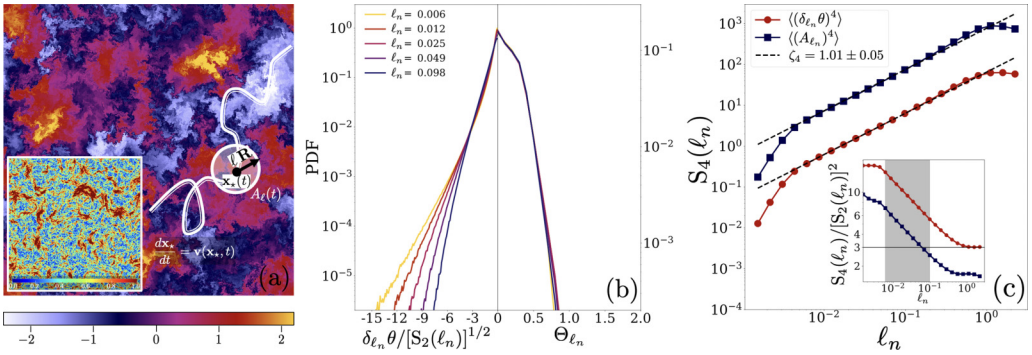

FIG. 1. Passive scalar in 2D inverse cascade: (a) Snapshot of the scalar field θ on a 4096^2 grid and (inset) of the velocity modulus $|\mathbf{v}|$. A sketch of the quasi-Lagrangian frame is represented by a Lagrangian trajectory (white curve), which solves $\frac{d\mathbf{x}_\star}{dt} = \mathbf{v}(\mathbf{x}_\star, t)$. At each time, scalar fluctuations $A_\ell(t)$ in Eq. (9) are defined around the center $\mathbf{x}_\star(t)$. (b) Probability density functions (PDFs) of (negative tails) normalized scalar increments, $\delta_{\ell_n}\theta/[S_2(\ell_n)]^{1/2}$ [with $S_p(\ell_n) = \langle(\delta_{\ell_n}\theta)^p\rangle$] and of (positive tail) the rescaled field, Θ_{ℓ_n}, at scale $\ell_n = 2^{-n}$, within the inertial range; notice that both fields are symmetric under a change of sign. The x and y axes are adjusted accordingly in each case. (c) Fourth-order structure function computed using scalar increments (red circles), $S_4(\ell_n) = \langle(\delta_{\ell_n}\theta)^4\rangle$, and amplitudes (9) (blue squares), $S_4^A(\ell_n) = \langle A_{\ell_n}^4\rangle$. Dashed lines indicate fitted slope, ζ_4, within the inertial range. The inset shows the kurtosis, $S_4(\ell_n)/[S_2(\ell_n)]^2$, as a function of ℓ_n for both quantities. The shaded region highlights the inertial range, where the statistical analysis of this study focuses.

where the characteristic time t_ℓ is given by

$$t_\ell = \ell/v_\ell, \quad v_\ell = v_{\ell_f}\,(\ell/\ell_f)^{1/3}, \tag{5}$$

with v_{ℓ_f} the characteristic velocity at the forcing scale ℓ_f. We then define the rescaled QL velocity field

$$\mathbf{V}_\ell(\mathbf{R}, \tau) = \delta_\ell \mathbf{v}(\mathbf{x}_\star(t), \mathbf{R}, t)/v_\ell. \tag{6}$$

Differentiating Eq. (6) with respect to τ and applying the incompressible 2D Euler equations [$\nu, \beta, \mathbf{f} = 0$ in Eq. (2)] for the inertial interval, yields

$$\partial_\tau \mathbf{V} + \mathbf{V}\cdot\nabla_\mathbf{R}\mathbf{V} = -\nabla_\mathbf{R} P + (\nabla_\mathbf{R} P)_{\mathbf{R}=0}, \quad \nabla_\mathbf{R}\cdot\mathbf{V} = 0, \tag{7}$$

where $\nabla_\mathbf{R}$ is the gradient in the space $\mathbf{R}$. The new pressure field $P(\mathbf{R}, \tau)$ is determined by the incompressibility condition, just as in the original Euler system. Equation (7) is invariant under the space-time scaling transformation

$$\mathbf{R},\ \tau,\ \mathbf{V} \mapsto \gamma\mathbf{R},\ \gamma^{2/3}\tau,\ \gamma^{1/3}\mathbf{V}, \tag{8}$$

which corresponds to the change of scale $\ell \mapsto \ell/\gamma$, that is why the subscript ℓ in $\mathbf{V}$ was omitted. The symmetry (8) is the precise mathematical formulation of the K41 theory, because the field $\mathbf{V}(\mathbf{R}, \tau)$ describes velocity increments and is unaffected by sweeping.

We now extend this approach to the scalar field. The QL scalar difference, $\delta_\ell\theta(\mathbf{x}_\star(t), \mathbf{R}, t)$, has the same intermittent statistics of the Eulerian increments. Thus, to obtain a nonintermittent field we need a suitable (nonlinear) normalization accounting for the local scalar activity. To this aim we introduce the scalar amplitude,

$$A_\ell(t) := \left(\frac{1}{\pi}\int_{|\mathbf{R}|\leqslant 1} [\delta_\ell\theta(\mathbf{x}_\star(t), \mathbf{R}, t)]^2 d^2\mathbf{R}\right)^{1/2}, \tag{9}$$

which we can write as $\langle[\delta_\ell\theta(\mathbf{x}_\star(t), \mathbf{R}, t)]^2\rangle_{\mathcal{D}_1}^{1/2}$, i.e., the root-mean-square scalar increment within the disk $\mathcal{D}_1 = \{\mathbf{R} : |\mathbf{R}| \leqslant 1\}$ centered at $\mathbf{x}_\star(t)$. Details on the way we computed the amplitudes A_{ℓ_n} can

be found in Appendix B. The amplitude $A_\ell(t)$ quantifies the average scalar fluctuations at scale ℓ and its moments $S_p^A(\ell_n) = \langle A_{\ell_n}^p \rangle$ scale as the standard structure functions, $S_p(\ell_n) = \langle (\delta_{\ell_n}\theta)^p \rangle$, as shown in Fig. 1(c) for $p = 4$ (analogous results hold for any p, not shown). The inset displays the flatness for both cases with, marked in gray, the inertial range considered in all the analysis discussed in this manuscript. We now introduce the rescaled passive scalar field

$$\Theta_\ell(\mathbf{R}, \tau) := \frac{\delta_\ell\theta(\mathbf{x}_\star(t), \mathbf{R}, t)}{A_\ell(t)} \tag{10}$$

that, as shown in Appendix C, obeys the equation

$$\partial_\tau\Theta + \mathbf{V}\cdot\nabla_{\mathbf{R}}\Theta - \Theta\langle\Theta\mathbf{V}\cdot\nabla_{\mathbf{R}}\Theta\rangle_{\mathcal{D}_1} = 0. \tag{11}$$

Equation (11) exhibits a hidden scaling symmetry under the change of variable (see Appendix D [33])

$$\Theta(\mathbf{R}, \tau) \mapsto \frac{\Theta(\mathbf{R}/\gamma, \tau/\gamma^{2/3})}{B_\gamma(\tau)}, \tag{12}$$

which combines K41 space-time scaling (8) with the nonlinear normalization $B_\gamma(\tau) = \langle\Theta^2(\mathbf{R}/\gamma, \tau/\gamma^{2/3})\rangle_{\mathcal{D}_1}^{1/2}$. This change of variables corresponds to the transformation $\ell \mapsto \ell/\gamma$ (Appendix E [33]), justifying the term scaling symmetry and the omission of subscript ℓ in Θ and $\mathbf{V}$ in Eq. (11). The symmetry is hidden because it only manifests in the rescaled system: it emerges after normalizing the QL scalar increments by its local scalar amplitude, which defines the rescaled field in Eq. (10). Unlike the scaling relation $\theta \mapsto \gamma^\alpha\theta$ for the original scalar field, where α is arbitrary, HS (12) has no free parameter.

Summarizing, the recovery of hidden scaling symmetry implies that the field Θ is statistically self-similar:

$$\Theta_\ell \overset{\text{law}}{=} \Theta_{\ell'}, \quad \text{for } \ell \text{ and } \ell' \text{ in the inertial interval.} \tag{13}$$

This is verified on the right of Fig. 1(b), showing the collapse of the PDFs of Θ_ℓ for ℓ within the inertial range (compare with the left of the figure showing the original, unrescaled, increments). Actually, Eq. (13) has more general consequences, as it implies that the statistics of any observable of Θ is independent of the scale. As shown below, this has important implications with respect to the validity of (i) the third Kolmogorov hypothesis on the universality of multiplier statistics [24,25] (whose definition is here extended to the passive scalar field) and (ii) the Perron-Frobenius framework for the anomalous scaling of structure functions [18,27].

We conclude this section by noting that if we were instead analyzing the velocity field in the 3D forward cascade, the presence of intermittency, similarly to the passive scalar case, would require a nonlinear transformation of the velocity field, involving a normalization by the local velocity fluctuations [20,34]. In that case, both the PDEs in Eqs. (7) and (11) would be modified accordingly. In this manuscript, however, we focus on the 2D inverse cascade, where the inertial range is more extended and which corresponds to the scenario where the zero-modes theory has already been tested [12].

IV. UNIVERSALITY OF MULTIPLIERS STATISTICS

The analog of Kolmogorov's multipliers for the original (not rescaled) scalar field can be defined as [24,25] $m_{\ell,\ell'}(\mathbf{x}, \mathbf{e}, \mathbf{e}', t) = |\delta_\ell\theta(\mathbf{x}, \mathbf{e}, t)|/|\delta_{\ell'}\theta(\mathbf{x}, \mathbf{e}', t)|$, where ℓ and ℓ' are scales from the inertial interval, and $\mathbf{e}$ and $\mathbf{e}'$ are direction vectors. Under the assumptions of spatial homogeneity and isotropy, the third Kolmogorov hypothesis [24] states that the multiplier statistics are universal and depend only on the scale ratio, $\gamma = \ell/\ell'$, and the angle between the direction vectors. By computing the multipliers in the QL frame, and multiplying and dividing by the same quantity $A_\ell(t)$, we can

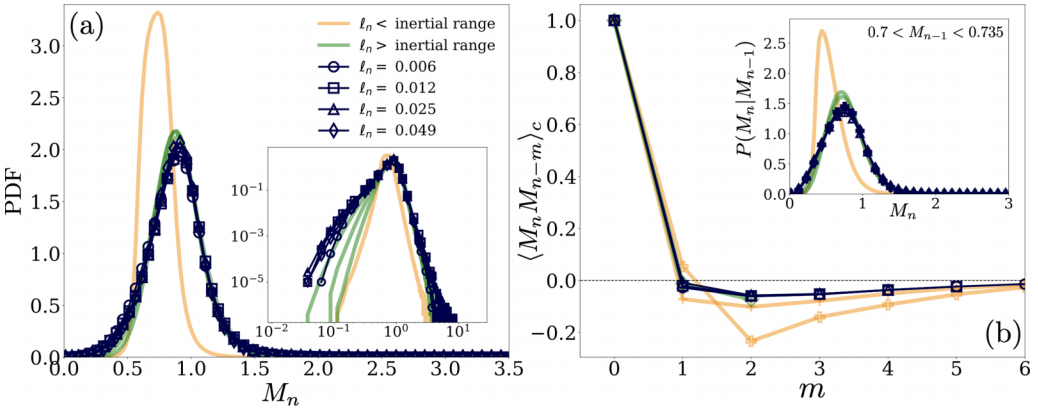

FIG. 2. (a) PDF of multipliers M_n at different scales $\ell_n = 2^{-n}$; (inset) same data in log-log scale. (b) Correlation function of multipliers, $\langle M_n M_{n-m} \rangle_c = (\langle M_n M_{n-m} \rangle - \langle M_n \rangle^2)/(\langle M_n^2 \rangle - \langle M_n \rangle^2)$. The inset presents the conditional distribution of multipliers between two consecutive scales, ℓ_n and ℓ_{n-1}, showing $P(M_n|M_{n-1})$ for a fixed interval $0.7 < M_{n-1} < 0.735$. In all panels, dark blue curves represent scales within the inertial range, while light orange and light green curves correspond to smaller and larger scales, respectively.

rewrite the multipliers as

$$m_{\ell,\ell'}(\mathbf{x}_\star(t), \mathbf{e}, \mathbf{e}', t) = \left| \frac{\Theta_\ell(\mathbf{e}, \tau)}{\Theta_\ell(\mathbf{e}'/\gamma, \tau)} \right|, \quad \ell/\ell' = \gamma. \tag{14}$$

The hidden scaling invariance of the rescaled field provides theoretical support to the third Kolmogorov hypothesis. In other words, multipliers statistics should depend on the scales ℓ and ℓ' only through their ratio γ, because the statistics of $\Theta_\ell(\mathbf{e}, \tau)$ is independent of ℓ [33].

Now, using our numerics, we scrutinize the multiplier statistics across different ℓ within the inertial range, while keeping $\gamma = \ell/\ell'$ fixed. It should be noted that the PDF of rescaled fields is peaked in $\Theta_\ell = 0$ [Fig. 1(b)]. This heavily influences the tails of PDFs for multipliers defined in (14), potentially leading to a misleading appearance of universality (see also discussion in [25]). To mitigate this problem we exploit Eq. (13) and consider multipliers defined in terms of scalar amplitudes [27], which are also expressed in terms of the rescaled field (Appendix F [33]):

$$M_n := \frac{A_{\ell_n}(t)}{A_{\ell_{n-1}}(t)} = \left\langle \Theta^2_{\ell_n}(\lambda \mathbf{R}, \tau) \right\rangle^{-1/2}_{\mathcal{D}_1}. \tag{15}$$

Here, M_n is the multiplier of scalar amplitudes between two consecutive scales ℓ_n and ℓ_{n-1}, where $\ell_n = \lambda^{-n}$. The last expression in Eq. (15) implies that universality of these multipliers follows from the HS. Furthermore, the integral in Eq. (15) has a low probability to be zero. We conducted tests using several values of $\lambda \in \{\sqrt{2}, 2, 2\sqrt{2}\}$ and found the results to be consistent with the theoretical predictions in all cases. The results shown below correspond to $\lambda = 2$. Figure 2(a) shows the PDF of the multiplier M_n defined at different scales ℓ_n, and their collpse when ℓ_n is within the inertial range. Moreover, the inset of Fig. 2(b) provides evidence of the collapse for inertial scales of the one-step conditional distribution of multipliers, $P(M_n|M_{n-1})$, at least for some values of M_{n-1}. Indeed from HS, we should expect not only the marginal distribution $P(M_n)$ to be independent of n [Fig. 2(a)], but also that the entire multipliers statistics is the same, provided inertial scales are considered. With our numerics we could investigate up to the conditional distribution, $P(M_n|M_{n-1}, M_{n-2})$, still verifying the universality (not shown).

V. PERRON-FROBENIUS (PF) SCENARIO TO ANOMALOUS SCALING

In the following, we show how Perron-Frobenius modes of a certain eigenvector measure, which emerges from the statistical hidden scaling symmetry, can be linked to the anomalous exponents. We start by noticing that the amplitude $A_{\ell_n} = M_n M_{n-1} \cdots M_1 A_{\ell_0}$ is obtained by the telescoping product of multipliers (15). We can then express the respective structure function

$$\mathrm{S}_p^A(\ell_n) := \langle A_{\ell_n}^p \rangle = \int d\mu_p^{(n)} \tag{16}$$

in terms of the measure

$$d\mu_p^{(n)} = P^{(n)}(M_n, \ldots, M_1) \prod_{k=1,n} M_k^p dM_k, \tag{17}$$

where, without lack of generality, we fixed the large scale amplitude $A_{\ell_0} = 1$. The joint probability of multipliers $P^{(n)}(M_n, \ldots, M_1)$ connects all scales, from ℓ_n in the inertial range to ℓ_0 in the forcing range. Consequently, the hypothesis of statistically restored HS (restricted to the inertial interval only) does not directly apply. Using Bayes theorem, we write $P^{(n)}(M_n, \ldots, M_1) = P^{(n)}(M_n|M_{n-1}, \ldots, M_1)P^{(n-1)}(M_{n-1}, \ldots, M_1)$. From this, we see that the measures (17) at different scales are connected by a linear operator

$$\mathcal{L}_p^{(n)} := M_n^p P^{(n)}(M_n|M_{n-1}, \ldots, M_1) dM_n \tag{18}$$

such that $d\mu_p^{(n)} = \mathcal{L}_p^{(n)}[d\mu_p^{(n-1)}]$ and, by recursion,

$$d\mu_p^{(n)} = \mathcal{L}_p^{(n)} \circ \mathcal{L}_p^{(n-1)} \circ \mathcal{L}_p^{(n-2)} \circ \cdots \circ \mathcal{L}_p^{(1)}\big[d\mu_p^{(0)}\big]. \tag{19}$$

In principle, every operator depends on both p and n. However, this dependence simplifies, i.e., the dependence on n disappears, in the inertial interval, where the HS predicts the universal joint statistics of multipliers. Additionally, Fig. 2(b) suggests that correlations between multipliers are local, i.e., decay at distant scales, while being noticeable across a few (at least four to five) scales. These arguments yield the inertial-range universality for conditional probabilities, $P^{(n)}(M_n|M_{n-1}, \ldots, M_1) \to P(M_n|M_{n-1}, \ldots)$ and, therefore, for the respective operators, $\mathcal{L}_p^{(n)} \to \mathcal{L}_p$.

The unique operator $\mathcal{L}_p$ governing the inertial range is a positive linear operator, mapping positive measure to positive measure. The Perron-Frobenius theorem ensures a unique maximum eigenvalue $\lambda_p > 0$ for this operator. Equation (19), reduced to repeated applications of the same $\mathcal{L}_p$, leads to the asymptotic form

$$d\mu_p^{(n)} = c_p \lambda_p^n d\nu_p, \tag{20}$$

where c_p is a positive (nonuniversal) coefficient accounting for large scales statistics and $d\nu_p$ is the eigenvector measure satisfying $\mathcal{L}_p[d\nu_p] = \lambda_p d\nu_p$ with the normalization $\int d\nu_p = 1$. Integration of (16) and (20) with $\ell_n = 2^{-n}$ yields

$$\mathrm{S}_p^A(\ell_n) = c_p \lambda_p^n = c_p \ell_n^{\zeta_p} \;\Rightarrow\; \zeta_p = -\log_2 \lambda_p. \tag{21}$$

We conclude that the PF framework expresses the scaling exponents ζ_p in terms of the eigenvalues λ_p. The PF scenario just described applies similarly to usual structure functions, $\mathrm{S}_p(\ell_n) = \langle (\delta_{\ell_n}\theta)^p \rangle$ as discussed in Appendix G [33].

To numerically verify the PF picture, two natural questions arise: how to estimate λ_p, and can we confirm the existence of the eigenvector measure $d\nu_p$? To address the first question, we estimated λ_p by considering three successive approximations of the operator $\mathcal{L}_p$ in (18). Here the full conditional probability is replaced by $P(M_n)$, $P(M_n|M_{n-1})$, or $P(M_n|M_{n-1}, M_{n-2})$; accounting for further correlations is computationally prohibitive. In the following we discuss how the approximated eigenvalues λ_p can be computed by solving an iterative linear problem for marginalized measures $d\mu_p^{(n)}$, with the results presented in Fig. 3(a).

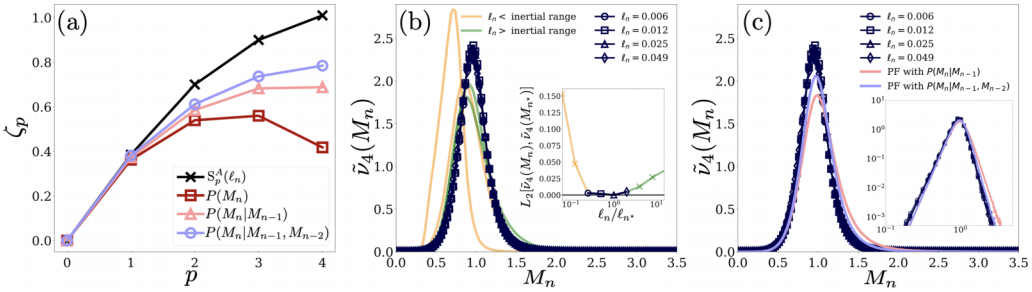

FIG. 3. (a) Comparison between anomalous exponents ζ_p for $p = 1, \ldots, 4$ fitted from the structure function $S_p^A(\ell_n) = \langle A_{\ell_n}^p \rangle$ and predicted by the Perron-Frobenious (PF) approach, Eq. (21), with three different approximations of the PF operator: using the measured marginal distribution $P(M_n)$ (not including correlations) or the conditional distributions $P(M_n|M_{n-1})$ and $P(M_n|M_{n-1}, M_{n-2})$, incorporating one- and two-step correlations (see legend). (b) Marginal eigenvector measure, $\tilde{\nu}_p(M_n)$, for $p = 4$ and different scales. In the inset, the distance in L_2 norm between marginal measures at different scales with respect to a fixed reference scale $\ell_{n^\star}$ in the inertial range: $L_2[\tilde{\nu}_p(M_n), \tilde{\nu}_p(M_{n^\star})]$. (c) Comparison of the eigenvector marginal measures $\tilde{\nu}_4(M_n)$, derived from the one-step and two-step multiplier correlations—$P(M_n|M_{n-1})$ and $P(M_n|M_{n-1}, M_{n-2})$ (represented by red and light blue curves, respectively, with $\ell_n = 0.025$ fixed)—and from the full statistics (dark blue curves). In the inset, the same plot in log-log scale.

We start with the uncorrelated case, where we assume that the variables M_n for different n are independent with the same probability distribution $P(M_n)$. In that case, expressions (16) and (17) yield

$$S_p^A(\ell_n) = c_p \langle M^p \rangle^n, \quad \langle M^p \rangle = \int M^p P(M) dM, \tag{22}$$

where $\langle M^p \rangle$ is a moment of every multiplier in the inertial interval and the coefficient c_p accounts for deviations from the universality in the forcing range. We recover the scaling (21) with $\lambda_p = \langle M^p \rangle$.

Next we consider the one-step conditional distribution $P(M_n|M_{n-1})$, which is an approximation of the full conditional distribution. As for the notation, we rewrite the measure in Eq. (17) as $d\mu_p^{(n)} = \mu_p^{(n)} dM_n \ldots dM_1$. This allows us to define the marginal measure $\tilde{\mu}_p^{(n)}(M_n)$ as follows:

$$\tilde{\mu}_p^{(n)}(M_n) = \int \mu_p^{(n)} dM_{n-1} \ldots dM_1 = \int M_n^p P(M_n|M_{n-1}) d\mu_p^{(n-1)}, \tag{23}$$

where we have skipped the integration by dM_n and where we have assumed $P(M_n|M_{n-1}, \cdots) \equiv P(M_n|M_{n-1})$. The marginal measure at the nth scale, $\tilde{\mu}_p^{(n)}$, is related to the marginal measure $\tilde{\mu}_p^{(n-1)}$ by

$$\tilde{\mu}_p^{(n)}(M_n) = \int M_n^p P(M_n|M_{n-1}) \tilde{\mu}_p^{(n-1)}(M_{n-1}) dM_{n-1}. \tag{24}$$

As $n \to \infty$, we expect the marginal measure to collapse to an eigenvectorlike form:

$$\tilde{\mu}_p^{(n)}(M_n) = c_p \lambda_p^n \tilde{\nu}_p(M_n), \tag{25}$$

where c_p is a constant and $\tilde{\nu}_p(M_n)$ is the marginal eigenvector measure associated with the eigenvalue λ_p. Substituting this into the recursive relation in Eq. (24), we get the following linear problem:

$$\lambda_p \tilde{\nu}_p(M_n) = \int M_n^p P(M_n|M_{n-1}) \tilde{\nu}_p(M_{n-1}) dM_{n-1}. \tag{26}$$

This is a standard eigenvalue problem, which can be solved numerically for λ_p.

Finally, we consider the case of a two-step conditional distribution, where $P(M_n|M_{n-1}, M_{n-2})$ is used instead of $P(M_n|M_{n-1})$. The corresponding marginal measures yield the following eigenvalue problem:

$$\lambda_p \tilde{\nu}_p(M_n, M_{n-1}) = \int M_n^p P(M_n|M_{n-1}, M_{n-2}) \tilde{\nu}_p(M_{n-1}, M_{n-2}) dM_{n-2}. \tag{27}$$

This equation is an iterative linear problem to be solved numerically for λ_p, where the marginal measure $\tilde{\nu}_p(M_n, M_{n-1})$ depends on two variables.

Despite the tested approximations are insufficient, there is a clear trend in Fig. 3(a): increasing knowledge of correlations improves the estimate. This suggests that including all essential correlations (up to five or more scales) would recover the correct scaling.

We now move to the second question, that is to verify the existence of the eigenvector measure $d\nu_p(M_n, M_{n-1}, \dots)$. Clearly, the full multidimensional verification is impractical. Instead, we check for the existence of the marginal eigenvector measure, $\tilde{\nu}_p(M_n) = \int \nu_p(M_n, M_{n-1}, \dots) dM_{n-1} \dots$, keeping only the dependence on M_n. From Eq. (20) and the normalization $\int d\tilde{\nu}_p = 1$, we write $\tilde{\nu}_p(M_n) = \tilde{\mu}_p^{(n)}(M_n)/\langle A_{\ell_n}^p \rangle$, where the marginal measure $\tilde{\mu}_p^{(n)}(M_n) = \langle A_{\ell_n}^p | M_n \rangle P(M_n)$ is expressed from Eq. (17), providing direct access to $\tilde{\nu}_p(M_n)$ from the simulation The existence of the eigenvector measure $d\nu_p$ guarantees that its marginal $\tilde{\nu}_p(M_n)$ is universal within the inertial range, as confirmed, e.g., for $p = 4$ in Fig. 3(b) showing the collapse at different scales ℓ_n. To better quantify the collapse, the inset of Fig. 3(b) shows the distances between the different curves by fixing a reference inertial scale, $\ell_{n^\star}$, and computing the L_2 norm between the marginal measure at each scale ℓ_n and the one at $\ell_{n^\star}$. In Fig. 3(c) we show the comparison between the marginal eigenvectors computed via full statistics and the eigenvectors obtained using the approximations of the PF operator in Eqs. (26) and (27). The eigenvectors of approximated PF operators demonstrate a clear convergence trend as the estimate of the PF operator improves. Similar convergence was observed for other orders of structure functions, such as $p = 3$ and 5.

VI. DISCUSSIONS

In this paper, we have shown that passive scalars advected by 2D turbulence in the inverse cascade possess a hidden symmetry. Such HS leads to a number of predictions, namely universality of the Kolmogorov multipliers (Fig. 2) and the link between Perron-Frobenius eigenvalues and anomalous exponents [Fig. 3(a)] and the fact that its (marginal) eigenvectors are well defined within the inertial range [Figs. 3(b) and 3(c)], which have been verified in high resolution numerical simulations of Eqs. (1) and (2). The hidden symmetry approach offers an alternative to zero-mode theory [4]. On the basis of our results along with previous works on shell models [19,21,27] and on NS equation [18,20,34], we conjecture that HS can offer a unified framework to interpret anomalous scaling in hydrodynamic field theory. This approach overcomes the main obstacle, which is the limitation of zero modes to the linear setting of turbulent transport. Understanding the links between hidden symmetry and zero modes (e.g., in the derivation of fusion rules [27,35–37]), with the possibility of extending them to NS and other models, revives and opens up directions for research into the theoretical foundations of developed turbulence. It will be interesting to investigate the HS for passive scalars advected by intermittent 3D turbulence. In the case of an active scalar, the symmetry group becomes smaller since the scalar does not scale independently of velocity. Exploring whether and how our approach extends to this case is another interesting direction for future research.

ACKNOWLEDGMENTS

The authors thank Guido Boffetta, Greg Eyink and Massimo Vergassola for useful discussion. This work was supported by the European Research Council (ERC) under the European Union's Horizon 2020 research and innovation programme (Grant Agreement No. 882340). A.A.M. was

also supported by CNPq Grant 308721/2021-7, FAPERJ Grant E-26/201.054/2022, and CAPES (Project MATH-AmSud CHA2MAN).

DATA AVAILABILITY

The data that support the findings of this article are openly available [38]; embargo periods may apply.

APPENDIX A: NUMERICAL SIMULATIONS

This Appendix details the DNS we implemented [13,15]. The numerical integration of the velocity field in Eq. (2) is performed using the 2D NS equation for vorticity ($\omega = \nabla \times \mathbf{v}$):

$$\frac{\partial \omega}{\partial t} + J(\omega, \Psi) = \nu \Delta^p \omega - \beta\omega - \Delta f_\omega, \tag{A1}$$

where Ψ is the stream function, and where the velocity field is given by $\mathbf{v} = \nabla^\perp \Psi = (\partial_y \Psi, -\partial_x \Psi)$. Here, $J(\omega, \Psi)$ represents the Jacobian determinant. The friction term $-\beta\omega$ extracts energy from the system at a characteristic friction scale $L_\beta \sim \epsilon^{1/2}\beta^{-3/2}$ with ϵ the energy flux toward the large scales, preventing large-scale energy accumulation. We force at small scales ℓ_{f_ω} with a Gaussian forcing with correlation function $\langle f_\omega(\mathbf{x}, t) f_\omega(\mathbf{0}, t')\rangle = \delta(t - t')\mathcal{F}_\omega(|\mathbf{x}|/\ell_{f_\omega})$ where $\mathcal{F}(x)$ rapidly decays for $\ell_n \gg \ell_{f_\omega}$ as $\mathcal{F}_\omega(x) = F_\omega \ell_{f_\omega}^2 \exp(-x^2/2)$. The inertial range for the inverse cascade of the velocity field is thus constrained between $\ell_{f_\omega} \ll \ell_n \ll L_\beta$. At small scales, enstrophy is dissipated by a hyperviscous term $\nu(-\Delta)^p\omega$ of order $p = 8$, as in [15]. The advection-diffusion equation (1) is forced at large scale L_θ with a Gaussian forcing, ensuring isotropic statistics, with zero mean and a correlation function $\langle f_\theta(\mathbf{x}, t) f_\theta(\mathbf{0}, t')\rangle = \delta(t - t')\mathcal{F}_\theta(x/L_\theta)$, and $\mathcal{F}_\theta$ has the same functional form of $\mathcal{F}_\omega$. The diffusive term in Eq. (1) is replaced by a bi-Laplacian operator, i.e., $\kappa(-\Delta)^2\theta$. In particular, we set $L_{f_\theta} \lesssim L_\beta$. Additionally, we impose $\ell_\kappa > \ell_{f_\omega}$, ensuring that the scalar is dissipated before reaching the forcing scale of the velocity field. These conditions are chosen to guarantee that the passive scalar dynamics evolve entirely within the inertial range of the velocity field. The numerical integration is carried out using a standard 2/3-dealiazed pseudospectral method on a doubly periodic square domain of size 4096×4096, with timestepping given by a second-order Adams-Bashforth scheme.

APPENDIX B: NUMERICAL COMPUTATION OF SCALAR AMPLITUDES

While the integral over the unit disk in Eq. (9) was convenient for the analytical derivation of the hidden symmetry, our theory is equally applicable if the averaging is performed over a different region. In our numerical analysis, we compute the average of scalar fluctuations over $K = 16$ discrete directions. Hence, A_ℓ is defined as

$$A_\ell = \sqrt{\sum_j [\theta(\mathbf{x} + \ell\hat{\mathbf{e}}_j) - \theta(\mathbf{x})]^2}, \tag{B1}$$

where the unit vectors $\hat{\mathbf{e}}_j$ are chosen as

$$\hat{\mathbf{e}}_j = \left(\cos\frac{2\pi j}{K}, \sin\frac{2\pi j}{K}\right), \quad j = 1, \ldots, K. \tag{B2}$$

The fact that we can equivalently use Eq. (9) or Eq. (B1) to define the scalar amplitudes stems from the generality of the theory: any positive functional $\mathcal{A}$ applied to the scalar field $\delta_\ell\theta(\mathbf{x}_\star(t), \mathbf{R}, t)$ that satisfies the homogeneity property $\mathcal{A}[c\delta_\ell\theta(\mathbf{x}_\star(t), \cdot, t)] = c\mathcal{A}[\delta_\ell\theta(\mathbf{x}_\star(t), \cdot, t)]$ for $c > 0$ can be considered. For a general description of the problem, in Eq. (9) we first defined the functional as the root-mean square of scalar fluctuations in the disk of radius 1, while Eq. (B1) revealed to be enough for practical purposes. This freedom of choice is further discussed in Ref. [20].

In our simulations, we tested different implementations of Eq. (B1), averaging the scalar fluctuations over varying numbers of directions (e.g., 2, 4, 8, 16, 32, and 64 directions). We verified that 16 was the optimal number of directions required to ensure reliable statistics and nonzero values in the denominator of the M_n multiplier. Increasing the number of directions does not improve the results.

Furthermore, for our single-time statistical analysis it is not necessary to switch to the QL frame to collect statistics on A_{ℓ_n}. Instead, the analysis can be performed directly in the Eulerian frame by averaging over the entire domain. This simplification is justified by the system's homogeneity and incompressibility, as is also true for the original multipliers in Eq. (14).

APPENDIX C: DERIVATION OF EQ. (11): EQUATIONS FOR THE IDEAL PASSIVE SCALAR SYSTEM

In this Appendix we present a step-by-step derivation of Eq. (11). Starting from Eq. (10) with $t = t_\ell \tau$, the chain rule yields

$$\partial_\tau \Theta_\ell = \frac{t_\ell}{A_\ell(t)} \frac{\partial}{\partial t} \delta_\ell \theta - t_\ell \frac{\delta_\ell \theta}{A_\ell^2(t)} \frac{dA_\ell}{dt}, \tag{C1}$$

where we used the shorthand $\delta_\ell \theta = \theta(\mathbf{x}_\star(t) + \ell \mathbf{R}, t) - \theta(\mathbf{x}_\star(t), t)$; notice that A_ℓ depends only on time. We now consider the first term of the equations (C1), which can be written as

$$\frac{\partial}{\partial t} \delta_\ell \theta = \partial_t \theta(\mathbf{x}_\star(t) + \ell \mathbf{R}, t) - \partial_t \theta(\mathbf{x}_\star(t), t) + \frac{d\mathbf{x}_\star}{dt} \cdot \nabla \theta(\mathbf{x}_\star(t) + \ell \mathbf{R}, t) - \frac{d\mathbf{x}_\star}{dt} \cdot \nabla \theta(\mathbf{x}_\star(t), t). \tag{C2}$$

Here the expressions $\partial_t \theta(\mathbf{x}_\star(t) + \ell \mathbf{R}, t)$ and $\nabla \theta(\mathbf{x}_\star(t) + \ell \mathbf{R}, t)$ denote the derivatives $\partial_t \theta$ and $\nabla \theta$ evaluated at $\mathbf{x} = \mathbf{x}_\star(t) + \ell \mathbf{R}$. Similarly, we express

$$\nabla_{\mathbf{R}} \Theta_\ell = \frac{\ell}{A_\ell(t)} \nabla \theta(\mathbf{x}_\star(t) + \ell \mathbf{R}, t). \tag{C3}$$

Using the ideal transport equation $\partial_t \theta = -\mathbf{v} \cdot \nabla \theta$ and the definition $d\mathbf{x}_\star/dt = \mathbf{v}(\mathbf{x}_\star(t), t)$ of the Lagrangian tracer, Eq. (C2) after a cancellation of two terms becomes

$$\frac{\partial}{\partial t} \delta_\ell \theta = -\mathbf{v}(\mathbf{x}_\star(t) + \ell \mathbf{R}, t) \cdot \nabla \theta(\mathbf{x}_\star(t) + \ell \mathbf{R}, t) + \mathbf{v}(\mathbf{x}_\star, t) \cdot \nabla \theta(\mathbf{x}_\star(t) + \ell \mathbf{R}, t). \tag{C4}$$

From definitions (5) and (6) we have

$$\mathbf{v}(\mathbf{x}_\star(t) + \ell \mathbf{R}, t) - \mathbf{v}(\mathbf{x}_\star(t), t) = \frac{\ell}{t_\ell} \mathbf{V}_\ell(\mathbf{R}, \tau). \tag{C5}$$

Using Eqs. (C3) and (C5), we reduce Eq. (C4) to the form

$$\frac{t_\ell}{A_\ell(t)} \frac{\partial}{\partial t} \delta_\ell \theta = -\mathbf{V}_\ell \cdot \nabla_{\mathbf{R}} \Theta_\ell. \tag{C6}$$

The time derivative of $A_\ell(t)$ is expressed from the definition (9) as

$$\frac{dA_\ell}{dt} = \frac{1}{A_\ell(t)} \left\langle \delta_\ell \theta \frac{\partial}{\partial t} \delta_\ell \theta \right\rangle_{\mathcal{D}_1}. \tag{C7}$$

Using Eq. (C6) and expressing $\delta_\ell \theta / A_\ell(t) = \Theta_\ell(\mathbf{R}, \tau)$ from Eq. (10), we find

$$\frac{t_\ell}{A_\ell(t)} \frac{dA_\ell}{dt} = -\langle \Theta_\ell \mathbf{V}_\ell \cdot \nabla_{\mathbf{R}} \Theta_\ell \rangle_{\mathcal{D}_1}. \tag{C8}$$

Using expressions (C6), (C8), and Eq. (10) in Eq. (C1) yields Eq. (11).

We note that A_ℓ in principle depends on both $\mathbf{x}_\star$ and t, however, the QL system (7) gains a new symmetry related to a change of the tracer. Considering any tracer $\mathbf{R}_\star(\tau)$ of the QL velocity, which satisfies the equation $\frac{d\mathbf{R}_\star}{d\tau} = \mathbf{V}(\mathbf{R}_\star, \tau)$. One can check that system is invariant under the

transformation $\mathbf{R},\ \tau,\ \mathbf{V} \mapsto \mathbf{R} - \mathbf{R}_\star(\tau),\ \tau,\ \mathbf{V} - \mathbf{V}_\star(\tau)$, where $\mathbf{V}_\star(\tau) = \mathbf{V}(\mathbf{R}_\star(\tau), \tau)$. One can see that this transformation corresponds to a change of tracer in the original coordinates [32].

As a final remark, one should notice that while the original equation for the passive scalar (and equivalently its QL version for the scalar increments) was linear, the equation for the rescaled field [i.e., Eq. (11)] is nonlinear. Still it enjoys the hidden scaling symmetry, as derived in the next Appendix.

APPENDIX D: DEMONSTRATION THAT EQ. (11) IS INVARIANT UNDER THE CHANGE OF VARIABLE (8) AND (12): DERIVATION OF THE HIDDEN SYMMETRY

In this section we prove that the transformation in Eqs. (12) and (8) is indeed a symmetry for the rescaled passive scalar system, Eq. (11). Assuming that $\mathbf{V}(\mathbf{R}, \tau)$ and $\Theta(\mathbf{R}, \tau)$ satisfy Eq. (11), we have to show that the transformed fields

$$\mathbf{V}'(\mathbf{R}, \tau) = \gamma^{1/3}\mathbf{V}(\mathbf{R}/\gamma, \tau/\gamma^{2/3}), \quad \Theta'(\mathbf{R}, \tau) = \frac{\Theta(\mathbf{R}/\gamma, \tau/\gamma^{2/3})}{B_\gamma(\tau)} \tag{D1}$$

solve the same equation, i.e.,

$$\partial_\tau \Theta' + \mathbf{V}' \cdot \nabla_{\mathbf{R}} \Theta' = \Theta' \langle \Theta' \mathbf{V}' \cdot \nabla_{\mathbf{R}} \Theta' \rangle_{\mathcal{D}_1}. \tag{D2}$$

Substituting Eq. (D1) into the lhs of Eq. (D2), after differentiation and dropping the common factor, we have

$$\frac{\Theta_\tau + \mathbf{V} \cdot \nabla_{\mathbf{R}} \Theta}{\gamma^{2/3} B_\gamma(\tau)} - \frac{\Theta}{B_\gamma^2(\tau)} \frac{dB_\gamma}{d\tau} = \frac{\Theta \langle \Theta \mathbf{V} \cdot \nabla_{\mathbf{R}} \Theta \rangle_{\mathcal{D}_1}}{\gamma^{2/3} B_\gamma^3(\tau)}, \tag{D3}$$

where all fields in the numerators are evaluated at $(\mathbf{R}/\gamma, \tau/\gamma^{2/3})$. Using Eq. (12) in the first term and then multiplying by $-\gamma^{2/3} B_\gamma^3/\Theta$, we further write

$$\gamma^{2/3} B_\gamma(\tau) \frac{dB_\gamma}{d\tau} + \left(1 - B_\gamma^2(\tau)\right) \langle \Theta \mathbf{V} \cdot \nabla_{\mathbf{R}} \Theta \rangle_{\mathcal{D}_1} = 0. \tag{D4}$$

Expressing $B_\gamma(\tau) = \langle \Theta^2(\mathbf{R}/\gamma, \tau/\gamma^{2/3}) \rangle_{\mathcal{D}_1}^{1/2}$, we have

$$\langle \Theta \partial_\tau \Theta \rangle_{\mathcal{D}_1} + (1 - \langle \Theta^2 \rangle_{\mathcal{D}_1}) \langle \Theta \mathbf{V} \cdot \nabla_{\mathbf{R}} \Theta \rangle_{\mathcal{D}_1} = 0, \tag{D5}$$

recalling that all fields assume the argument $(\mathbf{R}/\gamma, \tau/\gamma^{2/3})$. This equation coincides with Eq. (11) multiplied by Θ and averaged over the disk $\mathcal{D}_1$, therefore, proving Eq. (D2).

APPENDIX E: DEMONSTRATION THAT THE HIDDEN SYMMETRY CORRESPONDS TO A SCALING SYMMETRY

Now let us show that the hidden symmetry relates the two scales, ℓ and $\ell' = \ell/\gamma$. Namely, we will prove that the relations (12) transform the respective rescaled field $\Theta_\ell(\mathbf{R}, \tau)$ to $\Theta_{\ell'}(\mathbf{R}', \tau')$, where the primes remind that the rescaled variables (4) depend on the reference scale ℓ'. Expressing

$$\delta_{\ell'} \theta(\mathbf{x}_\star(t), \mathbf{R}', t) = \delta_\ell \theta(\mathbf{x}_\star(t), \mathbf{R}'/\gamma, t) \tag{E1}$$

from Eq. (3), we write the amplitude (9) at scale ℓ' as

$$A_{\ell'}(t) = \left(\frac{1}{\pi} \int_{|\mathbf{R}'| \leqslant 1} [\delta_\ell \theta(\mathbf{x}_\star(t), \mathbf{R}'/\gamma, t)]^2 d^2\mathbf{R}' \right)^{1/2}. \tag{E2}$$

Dividing by $A_\ell(t)$ and recalling definition (10) yields

$$\frac{A_{\ell'}(t)}{A_\ell(t)} = \left(\frac{1}{\pi} \int_{|\mathbf{R}'| \leqslant 1} \Theta_\ell^2(\mathbf{R}'/\gamma, \tau) d^2\mathbf{R}' \right)^{1/2}, \tag{E3}$$

where $\tau = t/t_\ell$. Similarly, using the definition (10) and the identity (E1), we express

$$\Theta_{\ell'}(\mathbf{R}', \tau') = \frac{\delta_\ell \theta(\mathbf{x}_\star(t), \mathbf{R}'/\gamma, t)}{A_\ell(t)} \frac{A_\ell(t)}{A_{\ell'}(t)}, \tag{E4}$$

where we also multiplied and divided by the same quantity $A_\ell(t)$. Using Eqs. (10) and (E3) in Eq.(E4) we derive

$$\Theta_{\ell'}(\mathbf{R}', \tau') = \frac{\Theta_\ell(\mathbf{R}'/\gamma, \tau'/\gamma^{2/3})}{\left(\frac{1}{\pi}\int_{|\mathbf{R}'|\leqslant 1} \Theta_\ell^2(\mathbf{R}'/\gamma, \tau'/\gamma^{2/3}) d^2\mathbf{R}'\right)^{1/2}}, \tag{E5}$$

where we also substituted $\tau = \tau'/\gamma^{2/3}$ following from the scaling relations (4) and (5). This is the hidden symmetry transformation (12).

APPENDIX F: DERIVATION OF EQ. (15)

Relation (15) follows from Eqs. (9) and (10) as

$$\begin{aligned} M_n &= \left(\frac{A_{\ell_{n-1}}(t)}{A_{\ell_n}(t)}\right)^{-1} = \left(\frac{1}{\pi A_{\ell_n}^2(t)} \int_{|\mathbf{R}|\leqslant 1} [\delta_{\ell_{n-1}}\theta(\mathbf{x}_\star(t), \mathbf{R}, t)]^2 d^2\mathbf{R}\right)^{-1/2} \\ &= \left(\frac{1}{\pi}\int_{|\mathbf{R}|\leqslant 1} \left[\frac{\delta_{\ell_n}\theta(\mathbf{x}_\star(t), \lambda\mathbf{R}, t)}{A_{\ell_n}(t)}\right]^2 d^2\mathbf{R}\right)^{-1/2} = \left(\frac{1}{\pi}\int_{|\mathbf{R}|\leqslant 1} \Theta_{\ell_n}^2(\lambda\mathbf{R}, \tau) d^2\mathbf{R}\right)^{-1/2}, \end{aligned} \tag{F1}$$

where we also used Eq. (3) with $\ell_{n-1} = \lambda\ell_n$.

APPENDIX G: PERRON-FROBENIUS SCENARIO FOR OTHER STRUCTURE FUNCTIONS

Here we show that the Perron-Frobenius approach can be extended to other definitions of the structure functions, including the usual one in terms of scalar increments from Eq. (3), namely, the moments $\langle|\delta_\ell\theta(\mathbf{x}, \mathbf{e}, t)|^p\rangle$. We write these increments in terms of the multipliers (15) and the rescaled field (10) as

$$|\delta_{\ell_n}\theta(\mathbf{x}_\star(t), \mathbf{e}, t)|^p = |\Theta_{\ell_n}(\mathbf{e}, \tau)|^p M_n^p \cdots M_1^p A_{\ell_0}^p. \tag{G1}$$

Using the measure (16), we express the respective structure function as

$$\langle|\delta_{\ell_n}\theta|^p\rangle = \int Q^p P_Q^{(n)}(Q|M_n, M_{n-1}, \ldots)\, dQ\, d\mu_p^{(n)}, \tag{G2}$$

where $P_Q^{(n)}(Q|M_n, M_{n-1}, \ldots)$ is the conditional probability density of $Q = |\Theta_{\ell_n}(\mathbf{e}, \tau)|$. Assuming that $P_Q^{(n)}$ is scale-local (thus, depending only on the scales from the inertial interval), the hidden scaling symmetry ensures that $P_Q^{(n)} = P_Q$ does not depend on n. Finally, using the Perron-Frobenius asymptotics (19), similarly to Eq. (20), we derive

$$\langle|\delta_{\ell_n}\theta|^p\rangle = q_p c_p \ell_n^{\zeta_p}, \quad \zeta_p = -\log_\lambda \lambda_p, \tag{G3}$$

where $q_p = \int Q^p P_Q(Q|M_n, M_{n-1}, \ldots)\, dQ\, d\nu_p$. We obtained the scaling law with the same exponent ζ_p but a different constant prefactor q_p.

[1] F. Pasquill and F. B. Smith, *Atmospheric Diffusion* (Ellis Horwood Chichester, New York, NY, 1983), Vol. 437.

[2] F. A. Williams, *Combustion Theory* (CRC Press, Boca Raton, 2018).

[3] B. I. Shraiman and E. D. Siggia, Scalar turbulence, Nature (London) **405**, 639 (2000).
[4] G. Falkovich, K. Gawedzki, and M. Vergassola, Particles and fields in fluid turbulence, Rev. Mod. Phys. **73**, 913 (2001).
[5] R. H. Kraichnan, Anomalous scaling of a randomly advected passive scalar, Phys. Rev. Lett. **72**, 1016 (1994).
[6] K. Gawędzki and A. Kupiainen, Anomalous scaling of the passive scalar, Phys. Rev. Lett. **75**, 3834 (1995).
[7] M. Chertkov and G. Falkovich, Anomalous scaling exponents of a white-advected passive scalar, Phys. Rev. Lett. **76**, 2706 (1996).
[8] B. I. Shraiman and E. D. Siggia, Symmetry and scaling of turbulent mixing, Phys. Rev. Lett. **77**, 2463 (1996).
[9] A. Pumir, B. I. Shraiman, and E. D. Siggia, Perturbation theory for the δ-correlated model of passive scalar advection near the batchelor limit, Phys. Rev. E **55**, R1263 (1997).
[10] N. Antonov, Anomalous scaling regimes of a passive scalar advected by the synthetic velocity field, Phys. Rev. E **60**, 6691 (1999).
[11] A. Kupiainen and P. Muratore-Ginanneschi, Scaling, renormalization and statistical conservation laws in the kraichnan model of turbulent advection, J. Stat. Phys. **126**, 669 (2007).
[12] A. Celani and M. Vergassola, Statistical geometry in scalar turbulence, Phys. Rev. Lett. **86**, 424 (2001).
[13] A. Celani, A. Lanotte, A. Mazzino, and M. Vergassola, Universality and saturation of intermittency in passive scalar turbulence, Phys. Rev. Lett. **84**, 2385 (2000).
[14] A. Celani, A. Lanotte, A. Mazzino, and M. Vergassola, Fronts in passive scalar turbulence, Phys. Fluids. **13**, 1768 (2001).
[15] G. Boffetta, A. Celani, and M. Vergassola, Inverse energy cascade in two-dimensional turbulence: Deviations from gaussian behavior, Phys. Rev. E **61**, R29 (2000).
[16] U. Frisch, *Turbulence: The Legacy of AN Kolmogorov* (Cambridge University Press, 1995).
[17] A. Celani, M. Cencini, A. Mazzino, and M. Vergassola, Active and passive fields face to face, New J. Phys. **6**, 72 (2004).
[18] A. A. Mailybaev, Hidden spatiotemporal symmetries and intermittency in turbulence, Nonlinearity **35**, 3630 (2022).
[19] A. A. Mailybaev, Shell model intermittency is the hidden self-similarity, Phys. Rev. Fluids **7**, 034604 (2022).
[20] A. A. Mailybaev and S. Thalabard, Hidden scale invariance in navier–stokes intermittency, Philos. Trans. R. Soc. A **380**, 20210098 (2022).
[21] A. A. Mailybaev, Hidden scale invariance of turbulence in a shell model: From forcing to dissipation scales, Phys. Rev. Fluids **8**, 054605 (2023).
[22] Z.-S. She and E. Leveque, Universal scaling laws in fully developed turbulence, Phys. Rev. Lett. **72**, 336 (1994).
[23] B. Dubrulle, Intermittency in fully developed turbulence: Log-Poisson statistics and generalized scale covariance, Phys. Rev. Lett. **73**, 959 (1994).
[24] A. N. Kolmogorov, A refinement of previous hypotheses concerning the local structure of turbulence in a viscous incompressible fluid at high reynolds number, J. Fluid Mech. **13**, 82 (1962).
[25] Q. Chen, S. Chen, G. L. Eyink, and K. R. Sreenivasan, Kolmogorov's third hypothesis and turbulent sign statistics, Phys. Rev. Lett. **90**, 254501 (2003).
[26] G. Parisi and U. Frisch, *Turbulence and predictability in geophysical fluid dynamics: Proc. Intern. School of Physics 'Enrico Fermi', Varenna on Lake Como, Villa Monastero, 1983, Course LXXXIII* (North-Holland, 1985).
[27] S. Thalabard and A. A. Mailybaev, From zero-mode intermittency to hidden symmetry in random scalar advection, J. Stat. Phys. **191**, 131 (2024).
[28] A. Wirth and L. Biferale, Anomalous scaling in random shell models for passive scalars, Phys. Rev. E **54**, 4982 (1996).
[29] R. Benzi, L. Biferale, and A. Wirth, Analytic calculation of anomalous scaling in random shell models for a passive scalar, Phys. Rev. Lett. **78**, 4926 (1997).

[30] J. Paret and P. Tabeling, Intermittency in the two-dimensional inverse cascade of energy: Experimental observations, Phys. Fluids. **10**, 3126 (1998).
[31] G. Boffetta and R. E. Ecke, Two-dimensional turbulence, Annu. Rev. Fluid Mech. **44**, 427 (2012).
[32] V. I. Belinicher and V. S. L'vov, A scale-invariant theory of fully developed hydrodynamic turbulence, Sov. Phys. JETP **66**, 303 (1987).
[33] A subtle point in this derivation is that it is not automatically true that the single-point statistics in the Eulerian and QL frame coincide. The equivalence of the two statistics stems from the statistical homogeneity both in the Eulerian space and the space of initial Lagrangian states $\mathbf{x}_0 = \mathbf{x}_\star(0)$, together with incompressibility that ensures that the transformation $\mathbf{x}_0 \mapsto\!\!\to \mathbf{x} = \mathbf{x}_\star(t)$ has unit Jacobian at any fixed time.
[34] B. Magacho, S. Thalabard, M. Buzzicotti, F. Bonaccorso, L. Biferale, and A. A. Mailybaev, Scale invariance of intermittency in LES turbulence, J. Fluid Mech. **1016**, R5 (2025).
[35] G. L. Eyink, Renormalization group and operator product expansion in turbulence: Shell models, Phys. Rev. E **48**, 1823 (1993).
[36] R. Benzi, L. Biferale, and F. Toschi, Multiscale velocity correlations in turbulence, Phys. Rev. Lett. **80**, 3244 (1998).
[37] L. T. Adzhemyan, N. V. Antonov, V. A. Barinov, Y. S. Kabrits, and A. N. Vasil'ev, Calculation of the anomalous exponents in the rapid-change model of passive scalar advection to order ε^3, Phys. Rev. E **64**, 056306 (2001).
[38] C. Calascibetta, L. Biferale, F. Bonaccorso, and M. Cencini, TURB-Scalar. A large database of passive scalar fields advected by 2D Navier-Stokes in the turbulent inverse cascade regime, arXiv:2508.12762.